

**HOT WIRE ANEMOMETRY TECHNIQUES
ON A ROTATING TURBINE EXPERIMENTS**

**C.D. Sheldrake, R.W. Ainsworth
University of Oxford
England**

Hot-wire Anemometry Techniques on Rotating Turbine Experiments

C.D. Sheldrake, R.W. Ainsworth
Department of Engineering Science
University of Oxford

Abstract

This paper describes the use of hot-wires for making aerodynamic measurements in the rotor relative frame of reference. The technique provides a direct measurement, at high bandwidth, of turbine inlet Mach number distributions.

A standard hot-wire bridge coupled via slip rings to a rotating sensor can give rise to problems in obtaining reliable mean flow measurements because the coupling media itself can introduce spurious resistance changes into the bridge circuit. Such resistance changes can not only give rise to ambiguous calibrations, but will also have detrimental effects on the frequency response, signal to noise ratio and stability of the instrument. To overcome these difficulties a simple "in-shaft" constant temperature anemometer has been developed that can rotate with the turbine blade row, thus obviating any electro-mechanical interface between bridge components.

The rotor relative environment is harsh and the mean fluid properties are atypical of those encountered in the vast majority of hot-wire anemometry applications. Centripetal accelerations are also high; at design speed, for instance, the hot-wire sensors must be capable of withstanding angular accelerations of approximately 20,000g. The construction of rigid sensors is therefore prerequisite.

A method of *in situ* calibration at turbine representative conditions, using a compact, high contraction ratio nozzle is described. Results from a rotor relative rotor relative inlet survey using a miniature, blade mounted, mid height, single sensor hot-wire are presented and discussed in relation to CFD predictions.

Nomenclature

A, B	Constants
C	Capacitance
c	Specific heat capacity
E	Output voltage
H_f	Heat transfer coefficient
i	Current
L	Inductance
M	Mach Number
m	Mass
Nu	Nusselt Number
n	Exponent
P	Pressure
R	Resistance
Re	Reynolds Number
t	Time
T	Temperature
γ	Ratio of specific heats

Subscripts

f	Fluid
r	Sensor
w	Wire

Introduction

The Oxford Rotor Facility (Ainsworth *et al*, 1988) has been built to provide a simulation of conditions encountered in a modern rotating gas turbine stage. Using this facility an understanding of the complex flow phenomena maybe gained, and valuable data acquired for computational fluid dynamic (CFD) predictions. The blade profile being tested in the Oxford rotor has been studied in a two-dimensional linear cascade (Nicholson, J.H., 1981) and as part of a simulated wake and shock passing experiment, using a rotating bar arrangement (Doorly, D.J., 1985). In the present experiment, the Oxford Isentropic Light Piston Tunnel (ILPT) is configured as a 0.62 scale model turbine stage with highly instrumented turbine blades. Hot-wires mounted at mid height, on the leading edge are used to determine the rotor relative inlet Mach number distribution.

The Rotor Facility

The Oxford Rotor Facility consists of a single stage 0.5m diameter shroudless turbine attached to an ILPT, Figure 1. The pump tube contains a light piston, which is driven forward by high pressure air from a series of reservoirs, such that it

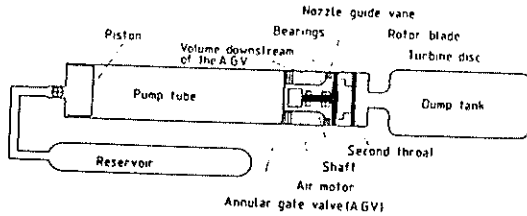


Figure 1. Layout of the ILPT

isentropically compresses the air ahead of it. When the desired total pressure is reached, a fast-acting annular gate valve, contained in a bolster plate, is opened (in approximately 30 ms) allowing high pressure air to enter the working section containing the turbine blade ring (60 blades) and nozzle guide vanes (36 blades). Before "firing" the tunnel the working section is evacuated to a pressure of about 20 KPa and the turbine spun up to a speed slightly less than design. The nature of the facility is transient, and as a consequence of the turbine being unbraked it accelerates rapidly through its design point during the 200ms run time.

Table 1

Mass Flow Number $\frac{\dot{m}\sqrt{T_0}}{P_0}$	7.04×10^{-4}
Specific Speed $\frac{N}{\sqrt{T_0}}$	436 rpm/K ^{1/2}
NGV Exit Mach Number	0.946
NGV Exit Reynolds Number	2.7×10^6
Upstream Total Pressure	8.02×10^5
Rotor Relative Exit Mach Number	0.959

The facility is able to simulate engine representative Mach and Reynolds number, as well as the relevant rotational groups. Details of the tunnel's operating point are shown above in Table 1.

Tunnel monitoring consists of both fast and slow data acquisition. Throughout the 200ms run

time quasi-steady temperatures, pressures, and the turbine speed, are sampled at 434 Hz, this data being predominantly used to determine the operating point. Fast data is obtained around the design point for approximately 15 ms at a sample rate of 500 kHz. A copper loom on the turbine disc connected to a slip ring allows signals from blade mounted transducers to be taken to the stationary frame.

Static and total pressures are measured at various positions throughout the rig. The working section is divided into a number of axial planes containing circumferential distributions of static pressure tappings. The "C" plane consist of 16 such tappings, on inner and outer annuli, that are positioned at NGV exit.

Hot-wire Anemometry

The hot-wire anemometer is basically a thermal transducer, the operation of which can best be viewed as a heat balance. The difference between the electrical heat supplied to the hot-wire and the heat transfer to the surrounding fluid will give rise to an enthalpy change:-

$$m_w c_w \frac{dT_w}{dt} = i^2 R_w - H_f \quad (1)$$

There are two modes of operating a hot-wire system. In the constant current mode the current flowing through the wire is kept constant - variations in the wire's resistance giving rise to a voltage drop variations across the wire. This system has largely been replaced with the superior constant temperature anemometer (CTA), which offers the major advantage of compensating, automatically, for changes in the thermal inertia of the filament. When using the hot-wire in constant temperature mode the element temperature is held approximately constant by a feedback loop such that the potential difference across the wire is controlled to maintain a predetermined sensor resistance. The filament is held at an elevated temperature and a temperature overheat ratio is defined as $(T_w - T_r)/T_r$. The overheat ratio used has implications on the frequency response of the anemometer; a higher overheat ratio will, in general, give rise to a higher frequency response.

The In-Shaft Anemometer Module

Operating a hot-wire in the rotating frame and monitoring the output signals in the stationary frame presents the user with two options; either the hot-wire and the coupling media must together form the bridge circuit, Figure 2, or the hot-wire and

anemometer must rotate together as one.

In the Oxford Rotor an air cooled 24 channel,

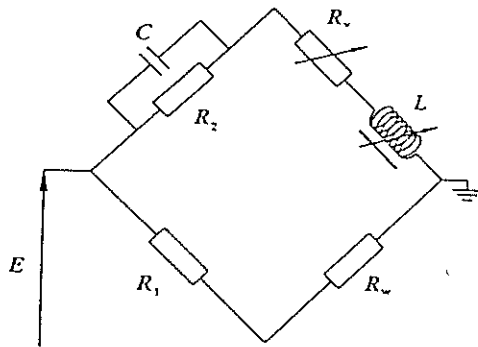


Figure 2. Hot-wire Wheatstone Bridge Circuit

silver plated contact slip ring, manufactured by IDM, type PM-24-01TC, is used to take measurements from the turbine blades. Previous studies on the characteristics of the slip rings have revealed that they exhibit speed and run time dependent resistance changes. These are of the order of 3% of the cold wire sensor resistance. If a hot-wire is operated through the slip ring then appreciable resistance changes of this order will have implications on the overall accuracy of the results. Firstly, a change in hot-wire resistance will alter the bridge voltage for a given flow regime and thus change the working overheat ratio. In other words the calibrated heat balance will be different from that of the experiment raising uncertainties on the validity of using the stationary calibration in any data analysis. Furthermore, the spurious resistance changes will detrimentally alter the instruments frequency response. Quite apart from the problem of any resistance change being introduced into the bridge from the slip rings is the problem of noise generation at the electro-mechanical interface. Small amounts of noise introduced here will be greatly amplified by the feedback loop and result in a much higher signal to noise ratio. It has been with these considerations in mind that has led to the design of a compact "in-shaft" anemometer module that can rotate with the turbine blade row and therefore maintain the integrity of the bridge circuit.

The "In-shaft" Electronics

The design of the anemometer follows along the familiar lines of using a differential input amplifier followed by a current amplifier to maintain a preset sensor resistance (Perry, A.E., 1982).

One of the chief requirements for the circuit, Figure 3, is that the thermal inertia of the hot-wire element and not the performance of the differential

amplifier should dictate the maximum attainable frequency response of the instrument. In terms of an operational amplifier specification this translates to a high slew rate.

The power-supply rejection ratio (PSRR), and to a lesser extent here, the common-mode rejection ratio (CMRR) are also important factors governing the performance of the amplifier. A high PSRR, typically >100 dB, will limit the effect of any noise generated in the power-supply lines, due to the slip rings, increasing the output signal noise. Insufficient CMRR will, effectively, introduce an output signal offset as a function of the DC input signal level. A high CMRR is obviously beneficial to circuit precision, although any errors introduced by a low CMRR should be accounted for in the hot-wire calibration procedure.

Here an OP-37 high speed, precision operational amplifier is used as the main amplifier. A Darlington amplifier then boosts the available current to the bridge and completes the feedback loop. Some of the important characteristics of the OP-37 are shown below in Table 2

Table 2

Slew Rate	17 V/ μ s
Gain Bandwidth, f_T	63 MHz
CMRR	114 dB
PSRR	100 dB
Noise @ 1kHz	3 nV/ \sqrt Hz

The passive components in the Wheatstone bridge arrangement are, to a large extent, particular to the operating range of the instrument and need to be chosen carefully. Resistors with a temperature coefficient no greater than 50 ppm/ $^{\circ}$ C should be used throughout so as to minimise temperature drift problems associated with electrical heating. In order to utilise the full DC voltage swing available to the bridge circuit the absolute values for the load and bias resistors, R_1 and R_2 need to be tailored to a nominal hot-wire resistance, overheat ratio, and calibration range. The resistances used here are 60 and 600 Ω for the load and bias resistors respectively. Three 6 watt, 180 Ω , 50 ppm/ $^{\circ}$ C, vitreous enamel resistors connected in parallel form the load resistor network - the high wattage and low temperature coefficient being essential for the temperature stability of the instrument.

The frequency response of the system is controlled by three main parameters:-

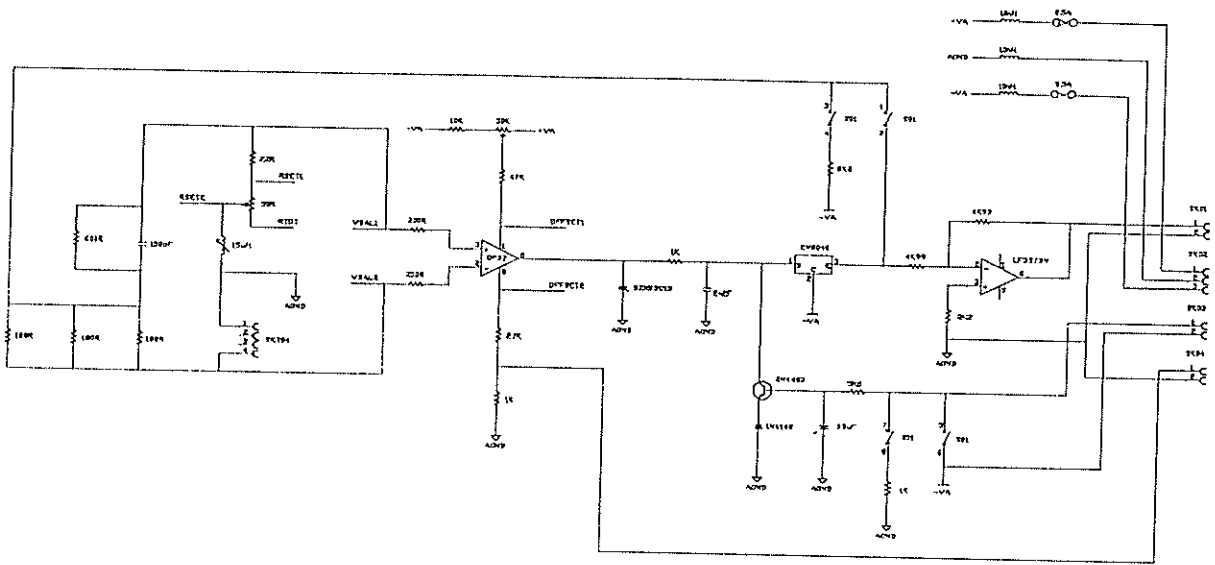


Figure 3. "In-shaft" Hot-wire Circuit Diagram

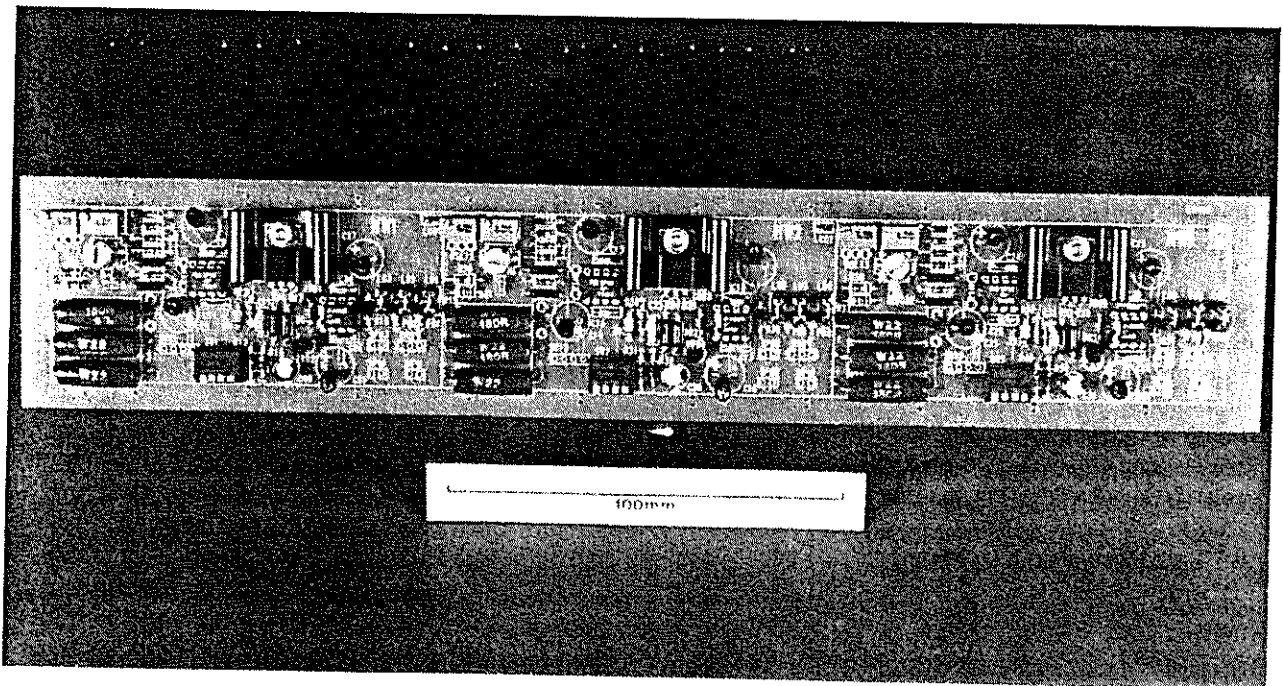


Figure 4. Photograph Of The "In-Shaft" Anemometer PCB

- Overheat ratio
- Bridge inductance/capacitance trimming
- Offset voltage

It is convenient to look at the influence of these variables in relation to the system transfer function, usually approximated to second order (Perry, A.E., Morrison, G.L., 1970), and the S-plane, Figure 5. System poles appearing in the left hand plane

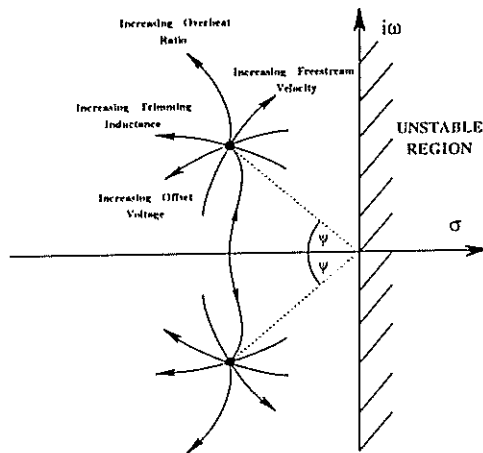


Figure 5. System Frequency Response

correspond to a frequency response consisting of exponentially decaying sinusoids, increasing in frequency the further away the poles are from the imaginary axis. Conversely, system poles situated in the right half plane refer to a frequency response of exponentially increasing sinusoids, and hence instability. The angle the poles subtend to the real axis defines the damping ratio of the system - the damping ratio reducing with angle, ϕ . Increasing the overheat ratio increases the system frequency response without altering the damping ratio appreciably. The effect of inductance in the bridge circuit has probably the most significance on amplifier performance (Perry, A.E., Morrison, G.L., 1970) - maybe as much as a fourfold increase in frequency response can be achieved by optimum trimming. Here a narrow range variable inductor (10-20 μ H) is used in conjunction with a fixed value capacitor (100pF) connected across the bias resistor to compensate for hot-wire cable inductance. These values are particular to the experiment and will be cable length, type, and geometry dependent. The offset voltage not only has a marked effect on the system stability, but it is also responsible for starting the amplifier controlling. Offset voltage is regulated by biasing the offset null connections of the OP-37. This also serves as a useful point for applying a pseudo error voltage to the input of the differential amplifier - the square wave test.

The physical dimensions of the "in-shaft" hot-wire anemometer board are dictated by the available space within the rotor shaft. As with the heat transfer circuit boards (Ainsworth *et al*, 1988) there is sufficient room for two 62mm by 300mm PCB's. Each PCB, Figure 4, consists of three electrically independent anemometer pods allowing a maximum of three hot-wires to be operated at any one time. This constraint is imposed by the number of slip ring channels available (each pod requires three power supply lines, two switch lines, two signal lines and a square wave test line).

Blade Mounted Hot-wires

A turbine blade has been adapted to carry a leading edge, mid height, hot-wire to record the freestream rotor relative inlet Mach number distribution. The chief design requirement for the blade was that the hot-wires must be able to be replaced without the need to remove the blade from the turbine blade row. This necessitates the use of a miniature plug and socket arrangement, whereby the hot-wire probe is the plug and the blade the socket.

The plug is a fabrication of five component parts and has the overall dimensions of 2.4mm in diameter and 12mm long. The hot-wire prongs are made from finely tapered 36 Gauge (ϕ 0.193mm) hard drawn stainless steel wire. This was used because of its high flexural rigidity and non-magnetic properties. The prongs are glued into a two hole ceramic tube (ϕ 1.2mm) and soldered to the plug end of the probe. The plug itself consists of two gold plated nickel rods (ϕ 0.5mm) restrained in a fibreglass body. A stainless tube is glued over the ceramic and fibreglass components to complete the hot-wire probe.

The socket is essentially the reverse of the plug. Two gold plated nickel rods are set into a fibreglass body, but these have full length axial holes that can accept the plug. Two wires are soldered to the outside of the socket and the whole let into the turbine blade. Figure 6 shows the single sensor hot-wire blade. The hot-wire can be removed from the blade, from suction surface to pressure surface, using an extractor that slides into the two axial holes in the socket.

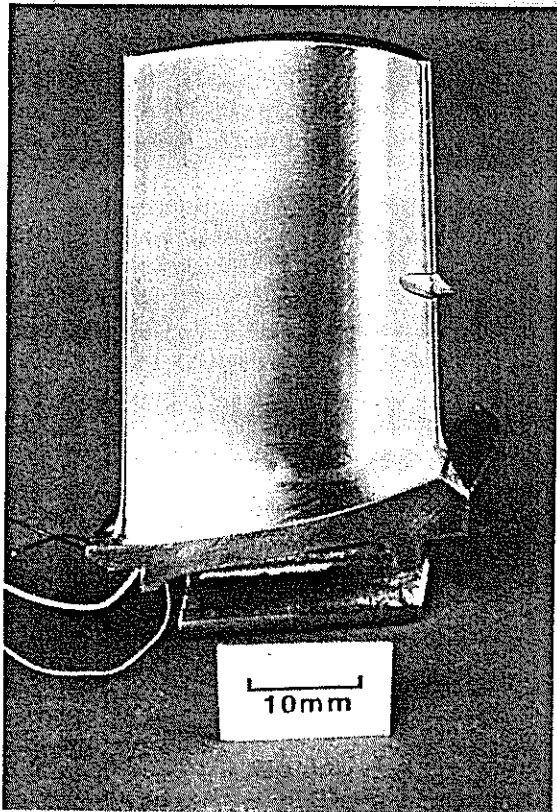


Figure 6. The Single Sensor Blade

Hot-wire Calibration Environment

The table below summarises the rotor relative environment. The values are based on an operating condition using a gas to wall temperature ratio of 1.3, and were obtained, or derived, from measurements taken in the facility.

Table 2

Total Pressure	5.05×10^5 Pa
Static Pressure	4.43×10^5 Pa
Total Temperature	327 K
Static Temperature	316 K
Static Density	5.14 kg/m^3
Inlet Mach Number	0.37

The nature of the flow parameters are different to those usually encountered in general hot-wire studies. The higher than ambient static density calls for a calibration in a variable density wind tunnel, or similar. There are two realistic options open for hot-wire probe calibration:-

- Remove the hot-wire probe, calibrate externally, then replace the probe
- In-situ calibration.

External calibration would involve using an identical circuit, fully matching all lead resistances, inductances and capacitances. There would also be uncertainty regarding the contact resistance of the probe and socket on reconnection.

To overcome these problems a compact, high contraction ratio, nozzle has been designed that can be fitted between inner and outer annuli upstream of the rotor.

The nature of the facility is such that the dump tank, and hence, working section may be raised above and lowered below atmospheric pressure. Inflating the dump tank to NGV exit static pressure and operating the nozzle within the working section will enable the fluid parameters, at the design point, to be matched as near as possible, Table 2.

Nozzle Design

The chief criteria for nozzle design are that the flow must not separate within the contraction and that the exit boundary layer thickness must not be too great. The design procedure used is based on the selection of two wall pressure coefficients (Morel T., 1975). These are chosen to avoid flow separation and produce the desired exit flow uniformity. Here, of course, there are physical constraints imposed upon the design. The geometrical factors limit the inlet diameter to 20mm. An exit diameter of 4mm was chosen giving a area contraction ratio of 25.

An arrangement of turbulence suppressing screens and gauges are positioned upstream of the nozzle contraction. These form a settling chamber and have the effect of providing the nozzle with a fairly uniform inlet flow. A photograph of the calibration nozzle is shown in Figure 7. A pressure tapping on the endwall, just upstream of the contraction, is used to measure the total pressure.

Hot-wire probe calibration

The calibration procedure for single and dual wire probes is essentially the same. The nozzle is positioned approximately one diameter away from the sensor plane, with its axis in line with the probe's axis. A reservoir containing high pressure air supplies the calibration nozzle and the resulting pressure drop across it is measured using a National piezoresistive transducer. The fluid's total temperature is simultaneously monitored using a K-type thermocouple. The calibration Mach number used here ranges from 0.3 to 0.55. The high Mach number condition is established initially, a valve in the reservoir supply line closed and the air pressure

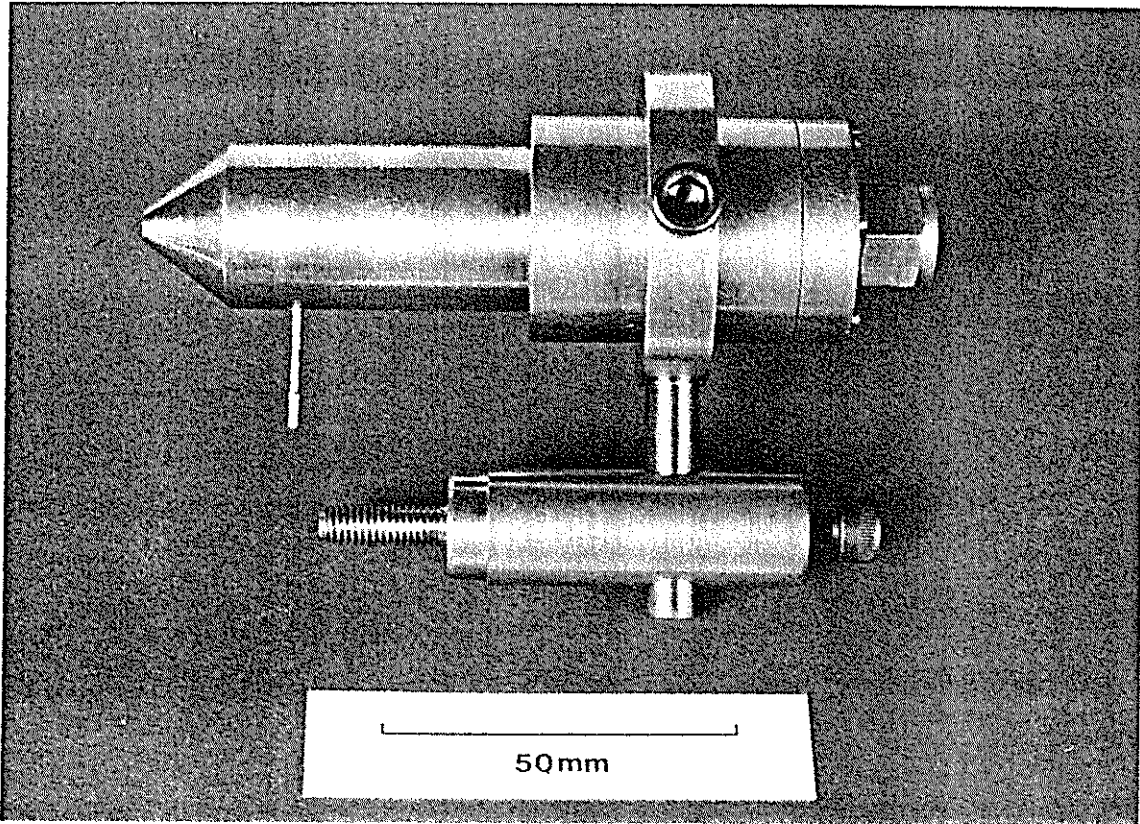


Figure 7. Photograph of the Calibration Nozzle

in the reservoir allowed to drop. This has the effect of reducing the pressure drop across the nozzle and hence exit Mach number. The output from the hot-

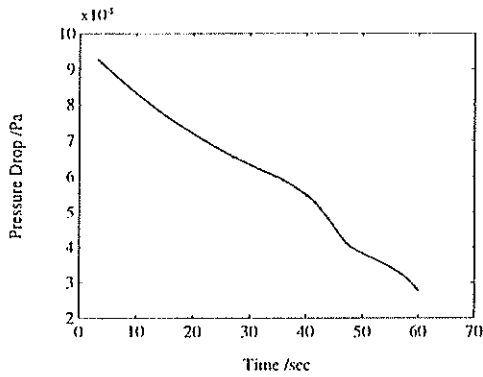


Figure 8. Nozzle Pressure Drop

wire probe together with the raw pressure drop and total temperature signals are fed into a transient recorder, sampling at 100Hz for the entire calibration run time of approximately 60 seconds. Figures 8, 9, and 10, show, respectively, the smoothed pressure drop and total temperature traces and the accompanying hot-wire output voltage.

The hot-wire output is corrected for any drift in

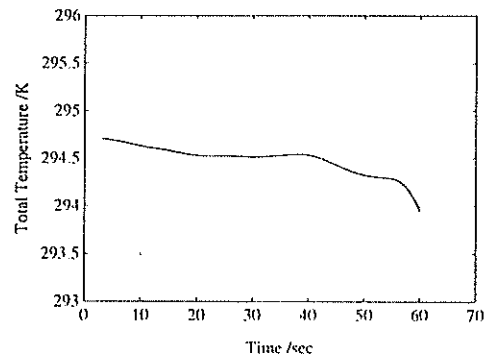


Figure 9. Calibration Total Temperature

the calibration total temperature (Kanevce, G., Oka, S., 1973) and normalised to a temperature of 289K. A heat balance according to King's law:-

$$Nu = A + BRe^n \quad (2)$$

is then applied to the data, each calibration being optimised, by varying the exponent, n , to produce the lowest normalised standard deviation. A typical

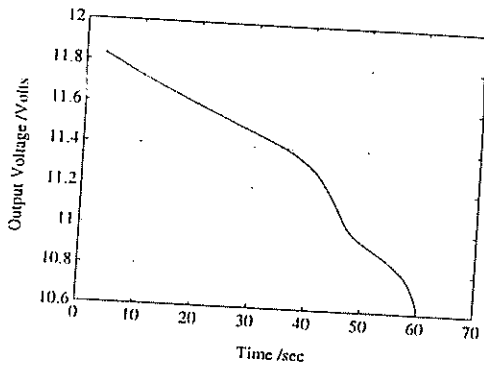


Figure 10. Hot-wire Calibration Curve

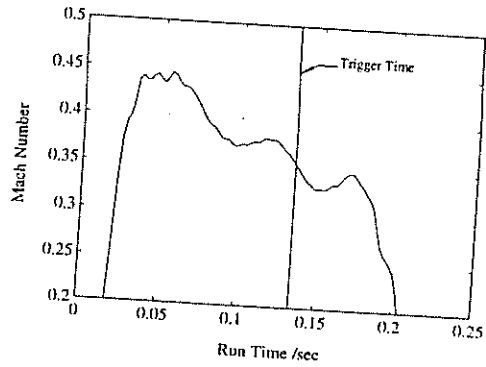


Figure 12. Rotor Relative Inlet Mach Number History

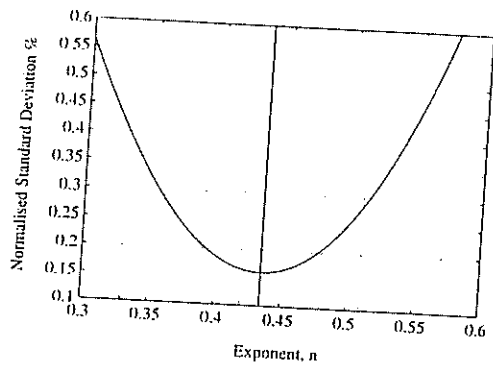


Figure 11. Calibration Optimisation Curve

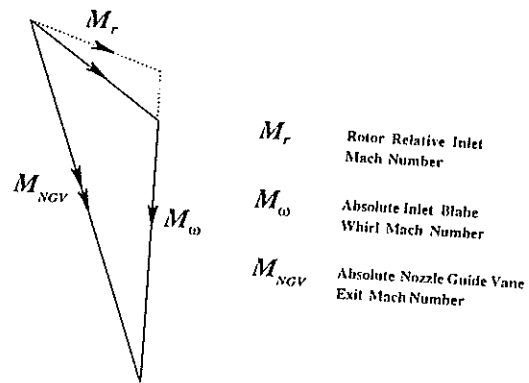


Figure 13. Rotor Inlet Velocity Triangle

optimisation curve is shown above, Figure 11.

Experimental results

Single hot-wire probes have been successfully tested in a rotor relative frame of reference in the Oxford Rotor facility. Figure 12 shows the rotor relative inlet Mach number history, sampled at 434 Hz, obtained from a single sensor probe throughout the duration of the run. The point in time during the run at which the transient recorders were triggered is also indicated.

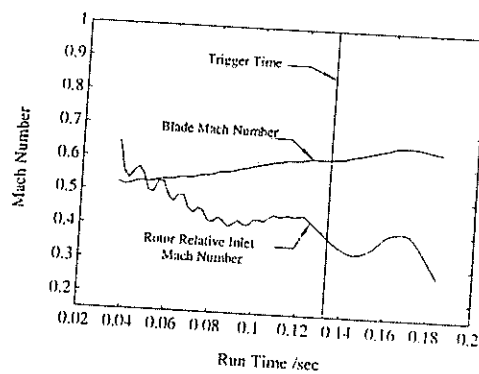


Figure 14. Derived Rotor Relative Inlet Mach Number

As previously mentioned the facility is transient in operation - the rotor accelerating through its design point. The effect of this can clearly be seen in the Rotor relative inlet Mach number history. A high rotor relative inlet Mach number is indicated immediately after the tunnel is fired (rotor speed approximately 6500 rpm) which then reduces as the run proceeds, this is predicted, qualitatively, from the inlet velocity triangle, Figure 13.

The rotor is also instrumented with a fast response, leading edge, rotor relative total pressure transducer (Kulite XCQ) positioned at mid-height. From the rotor relative inlet total pressure and an

average of the "C" plane static tapings an estimate of the mean rotor relative inlet Mach number, as a function of run time, can be obtained from:-

$$M(t) = \left(\frac{2}{\gamma - 1} \right)^{\frac{1}{2}} \left(\left(\frac{P_r(t)}{P_c(t)} \right)^{\frac{\gamma-1}{\gamma}} - 1 \right)^{\frac{1}{2}} \quad (3)$$

where P_r and P_c are the rotor relative total pressure and averaged "C" plane static pressures respectively. Figure 14 shows the derived rotor relative inlet Mach number, plotted with the blade Mach number.

Clearly there is excellent agreement between the two totally independent measures of Mach number, giving credence to the rotating hot-wire technique, and its use as an investigative tool.

The rotor is instrumented with three shaft encoders generating square wave pulses at the rotational frequency, and at 36 and 60 times the rotational frequency. The single line encoder is used to determine the angular position of the turbine blade row, the other two defining the wake passing frequency in the rotor relative frame of reference and at rotor exit.

The transient data, Figure 15, shows the rotor relative inlet Mach number obtained from the blade

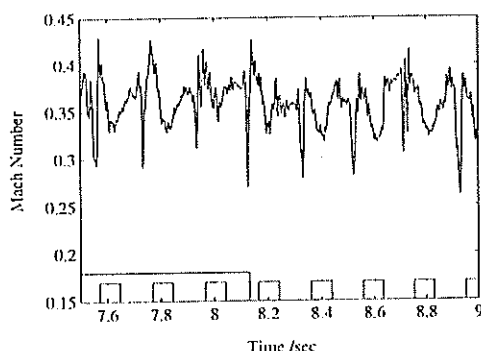


Figure 15. Rotor Relative Inlet Mach Number Distribution

mounted single sensor hot-wire sensor as it traverses the nozzle guide vane exit flow. The transient data are plotted together with the outputs from the 36 and one line shaft encoders. Very noticeable in the graphs are strong signs of a repeatable structure. There is a sharp drop in the inlet Mach number as the hot-wire probe traverses the NGV wake, followed by a relatively narrow peak, leading onto a trough and then a broader peak before the pattern repeats itself. The position of an NGV wake (one of the 36 per revolution of turbine) can be identified, from the physical geometry of the facility, as the instant in time when the output from the one line shaft encoder drops from logic high to

low. Looking at the resultant rotor relative inlet Mach number graphs this point correlates to the position of a narrow, sharp dip in the signal where the Mach number is approximately 30% lower than the time averaged mean value. This confirms what, heuristically, could be said to be the position of an NGV wake.

The origin of the mid passage drop in rotor relative inlet Mach number is thought to be due to the mixing of the core potential flow with the viscous layer - this type of flow interaction can be seen in the CFD animation.

Two dimensional CFD comparison

The computational code UNSFLO is a 2-D viscous, unsteady solver. It was developed by Dr Mike Giles (Giles, M.B., 1988) predominantly to analyse rotor/stator interaction. It has extremely novel and flexible features in the way in which it handles arbitrary stator/rotor pitch ratios, and incorporates highly accurate non-reflecting boundary conditions that minimise non-physical reflections at inflow and outflow boundaries.

The CFD predictions for rotor relative inlet Mach number is shown in Figure 16. The mean inlet Mach number is slightly below that suggested

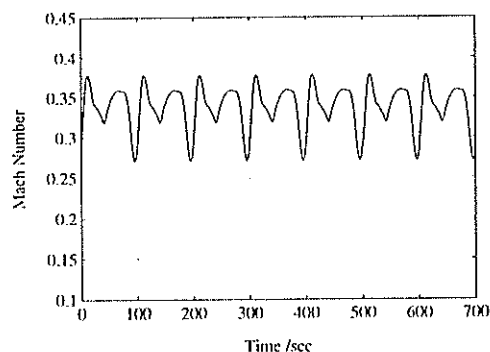


Figure 16. UNSFLO Prediction: Rotor Relative Inlet Mach Number Distribution

by the hot-wires and that derived from the relative total pressure measurements. The structure, however, depicts the same basic trends - there is the sharp drop in Mach number through the NGV wake and the same narrow and broad peaks on either side of the mid passage Mach number deficit. The perturbation of the CFD prediction is slightly lower in magnitude than the hot-wire result. It is evident, however, that the bandwidth of the CFD prediction is considerable lower than that of the experimental data.

Conclusion and Future Research Programme

The use of blade mounted hot-wires has been shown to be a valuable investigative tool for the rotor relative frame of reference. It can provide a direct measurement, at high bandwidth, of inlet Mach number distributions.

The construction of the hot-wire blades as a whole, used in conjunction with the "in-shaft" anemometer module and the *in situ* calibration nozzle has proved to be particularly successful. The ability to remove and replace the probe from the turbine blade with comparative ease, using the plug and socket arrangement, has lent itself to the technique.

The agreement obtained between the hot-wires, other independent measures, and the CFD solutions is seen as being most encouraging.

Future work will centre around obtaining a two dimensional picture of the freestream rotor relative inlet flow distribution using turbine blade mounted crossed hot-wires operated with the "in-shaft" anemometer module.

Acknowledgements

The authors would like to gratefully acknowledge the DRA Pyestock and Rolls-Royce plc for their support and permission to publish this paper. Thanks are also due to Kevin Grindrod for his enthusiasm in running the facility.

References

Ainsworth, R.W., Schultz, D.L., Davies, M.R.D., Forth, C.J.P., Hilditch, M.A., Oldfield, M.L.G. and Sheard, A.G., "A Transient Flow Facility for the Study of Thermofluid-Dynamics under Engine Representative Conditions". A.S.M.E. Paper 88-GT-144, 1988.

Doorly, D.J. and Oldfield, M.L.G., "Simulation of Wake Passing in a Stationary Turbine Rotor Cascade", Journal of Propulsion, pp 316-318, Vol. 1, No. 4, July 1985.

Giles, M.B., "Calculation of Unsteady Wake Rotor Interaction", AIAA Journal of Propulsion and Power, Vol4, pp356-362, 1988.

Kanevce, G. and Oka, S. "Correcting Hot-wire Readings for Influence of Fluid Temperature Variations". DISA Information No.15, pp 21-24, 1973.

Morel, T. "Comprehensive Design of Axisymmetric Wind Tunnel Contractions". Journal of Fluids Engineering, ASME Trans, pp 225-233, 1975.

Nicholson, J.H., "Experimental and Theoretical Studies of the Thermal Performance of Modern Gas Turbine Blades". D.Phil. Thesis, University of Oxford, United Kingdom, 1981.

Perry A.E., "Hot-wire Anemometry", Oxford Science Publications, Clarendon Press, Oxford,

1982.

Perry, A.E. and Morrison, G.L., "A Study of Constant-temperature Hot-wire Anemometry". Journal of Fluid Mechanics, Vol. 47, Part 3, pp 577-599, 1971.